DEPARTMENT OF MATHEMATICAL SCIENCES
SCHOOL OF SCIENCES AND HEALTH PROFESSIONS
OLD DOMINION UNIVERSITY
NORFOLK, VIRGINIA

BURGERS APPROXIMATION FOR TWO-DIMENSIONAL FLOW PAST AN ELLIPSE

By

J. Mark Dorrepaal, Principal Investigator

Progress Report
For the period May 26 - November 26, 1981

Prepared for the
National Aeronautics and Space Administration
Langley Research Center
Hampton, Virginia 23665

Under
Research Grant NAG1-197
Stephen F. Wornom, Technical Monitor
Transonic Aerodynamics Division

Submitted by the
Old Dominion University Research Foundation
P.O. Box 6369
Norfolk, Virginia 23508-0369

February 1982

TABLE OF CONTENTS

BURGERS APPROXIMATION FOR TWO-DIMENSIONAL FLOW PAST AN ELLIPSE

By

J. Mark Dorrepaal*

INTRODUCTION

Efforts during this phase of the research have concentrated on analyzing the Burgers flow past a circular cylinder, comparing predictions of the Burgers model with those of Oseen flow past a circle, and deriving exact solutions of the flow equations for elliptic geometries. The results are provided in the following sections of this report. The first section following the List of Symbols describes a motivation for studying Burgers flow. Then "Solution" outlines a solution technique which works equally well for Oseen or Burgers flow past a circular cylinder. This is followed by sections which describe the separation behind the cylinder, the drag experienced by the cylinder, and asymptotic behavior far from the cylinder. The section titled "Burgers Flow and Oseen Flow: How Do They Differ?" shows that the predictions of Burgers flow near the cylinder provide a substantial improvement over those of Oseen flow. Finally, "Burgers Flow Past an Elliptic Cylinder" gives the formulation and solution of the equations of motion for flow past an ellipse.

LIST OF SYMBOLS

a	cylinder radius
$A(\delta)$	coefficient in least squares fit
C_D	drag coefficient
E_n	coefficient in vorticity expansion

*Associate Professor, Department of Mathematical Sciences, Old Dominion University, Norfolk, Virginia 23508.

$F_n(r)$	radial eigenfunction resulting from separation of variables
$Gek_n\left(z, -\frac{1}{4}R^2\right)$	modified Mathieu function
$G(r,\theta;r_o,\theta_o)$	Green's function
$\hat{k}$	unit vector in z-direction
$K_n(x)$	modified Bessel function
$p(r,\theta)$	pressure
P	rear stagnation point of the cylinder
(r,θ)	polar coordinates
R	Reynolds number
R_c	critical minimum Reynolds number
R_s	Reynolds number based on the semimajor axis of the ellipse
$se_n(\theta, -\frac{1}{4}R^2)$	Mathieu function
$T_n(\theta)$	angular eigenfunction resulting from separation of variables
U	free-stream velocity
$\vec{v}$	fluid velocity
(x,y)	Cartesian coordinates
α	Reynolds number exponent in least squares fit
Γ_{kn}	coefficient in infinite linear system of equations
δ_{kj}	Kroneckar delta
$\delta(x)$	delta function
$\vec{\nabla}$	gradient operator
∇^2	Laplacian operator
(ξ,η)	elliptic coordinates for flow parallel to major axis
(μ,λ)	elliptic coordinates for flow perpendicular to major axis

ν	kinematic viscosity
ρ	fluid density
$\sigma_{rr}, \sigma_{r\theta}$	stress components
$\phi(r,\theta)$	harmonic conjugate of potential flow stream function
$\Phi_k(R)$	coefficient of higher order term in asymptotic expansion of stream function
$\chi(R)$	coefficient of second term in asymptotic expansion of stream function
$\chi(\mu,\lambda)$	stream function for potential flow past an ellipse perpendicular to its major axis
$\psi(r,\theta)$	stream function for Oseen or Burgers flow past a circle
$\psi(\xi,\eta)$	stream function for Burgers flow past an ellipse
$\Psi(\xi,\eta)$	stream function for potential flow past an ellipse parallel to its major axis
$\omega(r,\theta)$	vorticity

MOTIVATION

The nondimensional Navier-Stokes equation has the form

$$R(\vec{v} \cdot \vec{\nabla})\vec{v} = -\vec{\nabla}p + \nabla^2 \vec{v} \tag{1}$$

where R, $\vec{v}$, p are Reynolds number, fluid velocity, and pressure, respectively. The velocity vector must also satisfy the continuity equation

$$\vec{\nabla} \cdot \vec{v} = 0 \tag{2}$$

which is guaranteed if we use the following representation:

$$\vec{v} = \text{curl } \{\psi(r,\theta)k\} \tag{3}$$

where $\psi(r,\theta)$ is the stream function. By substituting equation (3) into equation (1) and eliminating $p(r,\theta)$, we can write the Navier-Stokes equation in the equivalent scalar form

$$\omega = -\nabla^2 \psi \tag{4}$$

$$\left[\nabla^2 + \frac{R}{r} D(\psi)\right]\omega = 0 \tag{5}$$

where

$$D(\psi) \equiv \frac{\partial \psi}{\partial r}\frac{\partial}{\partial \theta} - \frac{\partial \psi}{\partial \theta}\frac{\partial}{\partial r}$$

This suggests an iterative process

$$\left.\begin{aligned} \nabla^2 \psi_k &= -\omega_k \qquad (6) \\ \left[\nabla^2 + \frac{R}{r} D(\psi_k)\right]\omega_{k+1} &= 0 \qquad (7) \end{aligned}\right\} \quad k = 0,1,2,\ldots.$$

which defines a sequence $\{\psi_k(r,\theta)\}$ of spatially uniform approximations to the solution of equation (1). It is assumed that under appropriate conditions this sequence will converge to the solution of equation (1).

To begin the iterations we must propose initial values of $\omega_o(r,\theta)$ and $\psi_o(r,\theta)$ consistent with equation (6). Since we are considering uniform flow past a circular cylinder $r = 1$, the flow is irrotational at infinity and it is reasonable to choose $\omega_o(r,\theta) \equiv 0$. If we choose $\psi_o = r \sin\theta$, corresponding to a uniform stream, the problem for (ω_1, ψ_1) is Oseen flow. On the other hand, if we choose $\psi_o = (r - r^{-1}) \sin\theta$, corresponding to continuous inviscid flow past the cylinder, the resulting problem for (ω_1, ψ_1) is Burgers flow. Both flows should behave similarly at infinity. But in Oseen flow vorticity is convected through the cylinder while in Burgers flow it is convected around the cylinder. This suggests a difference in the two flows near the circle.

SOLUTION

With $k = 0$ and $\psi_0 = r \sin\theta$, equation (7) becomes the Oseen vorticity equation:

$$\left[\nabla^2 + R\,\frac{\sin\theta}{r}\,\frac{\partial}{\partial\theta} - R\cos\theta\,\frac{\partial}{\partial r}\right]\omega(r,\theta) = 0 \tag{8}$$

The Burgers vorticity equation has the form

$$\left[\nabla^2 + R\left(\frac{1}{r} + \frac{1}{r^3}\right)\sin\theta\,\frac{\partial}{\partial\theta} - R\left(1 - \frac{1}{r^2}\right)\cos\theta\,\frac{\partial}{\partial r}\right]\omega(r,\theta) = 0 \tag{9}$$

Both solutions are of the form

$$\omega(r,\theta) = -e^{\phi(r,\theta)} \sum_{n=1}^{\infty} E_n\, F_n(r)\, T_n(\theta) \tag{10}$$

where E_n are constants to be determined and ϕ, F_n, T_n are given in in table 1.

Table 1. functions occurring in vorticity expression.

Method	$\phi(r,\theta)$	$F_n(r)$	$T_n(\theta)$	
Oseen	$\frac{1}{2}$ Rr cos θ	$K_n\left(\frac{1}{2}\,Rr\right)$	sin n θ	
Burgers	R cosh z cos θ	$Gek_n\left(z, -\frac{1}{4}R^2\right)$	$se_n\left(\theta, -\frac{1}{4}R^2\right)$	z = ln r

The functions Gek_n and se_n are Mathieu functions, the former behaving asymptotically like exp (-R cosh z) as z = ln r → +∞, the latter being odd and periodic in θ with period 2π.

The stream function corresponding to $\omega(r,\theta)$ satisfies the Poisson equation (4) and the boundary conditions

$$\psi(1,\theta) = \frac{\partial \psi}{\partial r}(1,0) = 0 \tag{11}$$

A Green's function defined by

$$\nabla^2 G(r,\theta;r_o,\theta_o) = -\frac{1}{r}\delta(r - r_o)\,\delta(\theta - \theta_o) \tag{12}$$

$$G(r,\theta;1,\theta_o) = 0 \tag{13}$$

is used to solve for $\psi(r,\theta)$ with the result:

$$\psi(r_o,\theta_o) = (r_o - r_o^{-1})\sin\theta_o + \int_{-\pi}^{\pi}\int_1^{\infty} \omega(r,\theta) \cdot G(r,\theta;r_o,\theta_o) r\, dr\, d\theta \tag{14}$$

where

$$G(r,\theta;r_o,\theta_o) = -\frac{1}{4\pi}\ln\left[\frac{r^2 + r_o^2 - 2rr_o\cos(\theta - \theta_o)}{(rr_o)^2 + 1 - 2rr_o\cos(\theta - \theta_o)}\right]$$

To obtain the coefficients E_n in equation (10), we invoke the no-slip condition in equation (14):

$$0 = \frac{\partial \psi}{\partial r_o}(1,\theta_o) = 2\sin\theta_o + \int_{-\pi}^{\pi}\int_1^{\infty} \omega(r,\theta) \frac{\partial G}{\partial r_o}(r,\theta;1,\theta_o)\, r\, dr\, d\theta \tag{15}$$

Expanding $\frac{\partial G}{\partial r_o}$ in a Fourier sine series in θ_o and equating the resulting coefficients of $\sin k\theta_o$ $(k = 1,2,3,\ldots)$ on the right side of equation (15) to zero, we obtain an infinite linear system of the form

$$\sum_{n=1}^{\infty} E_n \Gamma_{kn} = \delta_{k1} \qquad k = 1,2,3,\ldots \tag{16}$$

where

$$\Gamma_{kn} = \frac{1}{\pi} \int_o^{\pi} \int_1^{\infty} r^{1-k} e^{1/2\, Rr \cos\theta} K_n\left(\frac{1}{2} Rr\right) \sin n\theta$$

$$\cdot \sin k\theta \, dr \, d\theta \qquad \text{(Oseen)}$$

$$\Gamma_{kn} = \frac{-1}{\pi} \int_o^{\pi} \int_o^{\infty} e^{(2-k)z + R \cosh z \cos\theta} \mathrm{Gek}_n\left(z, -\frac{1}{4} R^2\right)$$

$$\cdot \sin k\theta \; \mathrm{se}_n\left(\theta, -\frac{1}{4} R^2\right) dz \, d\theta \qquad \text{(Burgers)}$$

If equation (16) is truncated at $k = n = 8$, good results are obtained for Reynolds numbers in the range $0 < R \leq 4$.

SEPARATION

Both Oseen and Burgers flows exhibit separation on the downstream side of the cylinder provided the Reynolds number exceeds some critical minimum R_c. This value is found by solving the equation

$$\frac{\partial \omega}{\partial \theta}(1,0;R_c) = 0 \tag{17}$$

Yamada (ref. 1) has shown that $R_c = 1.51$ for Oseen flow and our calculations verify this result. For Burgers flow we find $R_c = 1.12$. A numeri-

cal value obtained by Underwood (ref. 2) from the Navier-Stokes equation is $R_c = 2.88$.

It is expected that the Burgers result would be less than the numerical value. The convective velocity field in Burgers flow is continuous inviscid potential flow past the cylinder, and this violates the no-slip condition at the cylinder's surface. The velocity field which solves the full Navier-Stokes equation satisfies this condition. Thus, convection effects near the cylinder are more dominant in Burgers flow than in Navier-Stokes flow, and any phenomena related to convection, such as separation, should occur at lower Reynolds numbers in Burgers flow.

The fact that the Burgers result is less than the Oseen value is a little surprising, but can be explained. Separation begins at the rear stagnation point P of the cylinder where locally the flow appears as in figure 1. At the onset of separation a bubble of circulating fluid forms about P. The direction of motion along the axis of symmetry inside the bubble is opposed to that outside the bubble (fig. 2). In Oseen flow the convective velocity field is constant in magnitude and perpendicular to the cylinder boundary in the vicinity of P as shown in figure 3. Oseen convection therefore will deter the establishment of reverse flow at P because it directly opposes the direction of fluid motion along the axis of symmetry inside the separation bubble. In contrast, the convective velocity field in Burgers flow is parallel to the cylinder boundary near P; in fact, its magnitude vanishes at the point P itself (fig. 4). Burgers convection does not oppose the establishment of a separation bubble about P in the way Oseen convection does, and we would therefore expect separation to initiate in Burgers flow at a lower Reynolds number.

As R increases beyond $R_c = 1.12$ in Burgers flow, the wake grows in size. When $R = 2.0$ the flow appears as in figure 5. The length of the wake is $PQ = 0.53$ where OP is the unit of length and $\angle SOP = 34.8°$. Point T, whose θ-coordinate is 83°, marks the location where the fluid pressure along the boundary is a minimum. The flow from T to S is against an adverse pressure gradient.

DRAG

A circular cylinder in a uniform stream experiences a force in the direction of the flow at infinity. The magnitude of this force is obtained by integrating the component of the stress vector in the direction of the uniform stream about the circumference of the circle. The drag is therefore

$$D = \rho\nu U \int_{-\pi}^{\pi} \left(\sigma_{rr} \cos\theta - \sigma_{r\theta} \sin\theta \right)_{r=1} d\theta \tag{18}$$

where σ_{rr}, $\sigma_{r\theta}$ are the stress components and ρ, ν, U are fluid density, kinematic viscosity, and free-stream velocity, respectively. The stress components can be calculated from equation (14) with the result

$$D = 2\rho\nu U \sum_{n=1}^{\infty} E_n \left[Gek_n\left(0, -\frac{R^2}{4}\right) - Gek_n'\left(0, -\frac{R^2}{4}\right) \right]$$

$$\cdot \int_{0}^{\pi} e^{R\cos\theta} \, se_n\left(\theta, -\frac{R^2}{4}\right) \sin\theta \, d\theta \tag{19}$$

The drag coefficient is defined to be

$$C_D = \frac{D}{(\rho U^2 a)} \tag{20}$$

where a is cylinder radius. Table 2 provides drag coefficients as computed from equation (19) for Reynolds numbers in the range $1 \leq R \leq 2$.

Table 2. Drag coefficients for $1 \leq R \leq 2$.

	R				
	1.0	1.12	1.25	1.50	2.0
C_D	7.76	7.29	6.86	6.22	5.35

These values agree well with the experiments of Tritton (see refs. 3 and 4). Table 2 will be expanded shortly to include Reynolds numbers in the range $1 \leq R \leq 4$ and drag coefficients for elliptic cylinders.

ASYMPTOTIC FORM OF FLOW FAR FROM CYLINDER

The solution of the full Navier-Stokes equation past a finite obstacle predicts a boundary layer surrounding the obstacle in which the flow is rotational and the velocity gradients are large. Outside this boundary layer the flow is essentially irrotational. Mathematically this means the stream function outside the boundary layer is harmonic. Since Oseen flow and Burgers flow are spatially uniform linear models of a Navier-Stokes flow, we would expect them both to exhibit this behavior.

If the Green's function $G(r,\theta;r_o,\theta_o)$ in equation (14) is expanded in a Fourier series, the coefficients of $\cos k\theta$ ($k = 1,2,\ldots$) all vanish, leaving the stream function in the following form:

$$\psi(r_o,\theta_o) = -\frac{1}{\pi}\sum_{k=1}^{\infty}\frac{1}{k}r_o^k \sin k\theta_o \int_o^{\pi}\int_1^{r_o} r^{1-k}\,\omega(r,\theta)\sin k\theta \, dr\, d\theta$$

$$+\frac{1}{\pi}\sum_{k=1}^{\infty}\frac{1}{k}r_o^{-k}\sin k\theta_o \int_o^{\pi}\int_1^{r_o} r^{1+k}\,\omega(r,\theta)$$

$$\cdot \sin k\theta \, dr\, d\theta \qquad (21)$$

This expression can in turn be written

$$\psi(r_o,\theta_o) = r_o \sin\theta_o - \sin\theta_o\left[\frac{\frac{1}{\pi}\int_o^{\pi}\int_1^{r_o}\omega(r,\theta)\sin\theta\, dr\, d\theta + 1}{r_o^{-1}}\right] \qquad (22)$$

(cont'd)

$$- \frac{1}{\pi} \sum_{k=2}^{\infty} \frac{1}{k} \sin k\theta_o \left[\frac{\int_0^{\pi} \int_1^{r_o} r^{1-k} \omega(r,\theta) \sin k\theta \, dr \, d\theta}{r_o^{-k}} \right]$$

$$+ \frac{1}{\pi} \sum_{k=1}^{\infty} \frac{1}{k} \sin k\theta_o \left[\frac{\int_0^{\pi} \int_1^{r_o} r^{1+k} \omega(r,\theta) \sin k\theta \, dr \, d\theta}{r_o^{k}} \right] \qquad (22)$$

(concl'd)

The three expressions in brackets in equation (22) all have finite limits as $r_o \to \infty$. Taking this limit, therefore, will yield the second term in the asymptotic expansion of the stream function far from the cylinder. The result is

$$\psi(r_o,\theta_o) \sim r_o \sin\theta_o - \frac{1}{\pi} \chi(R) \sum_{k=1}^{\infty} \frac{1}{k} \sin k\theta_o + O\left(\frac{1}{r_o}\right) \qquad (23)$$

Now it is known that

$$\sum_{k=1}^{\infty} \frac{1}{k} \sin k\theta_o = \frac{1}{2}(\pi - \theta_o) \qquad 0 < \theta_o < \pi \qquad (24)$$

$$= \frac{1}{2}(-\pi - \theta_o) \qquad -\pi < \theta_o < 0 \qquad (25)$$

Thus the stream function has the asymptotic form

$$\psi(r_o,\theta_o) \sim r_o \sin\theta_o - \frac{1}{2} \chi(R) \left(\pm 1 - \frac{\theta_o}{\pi}\right) + O(r_o^{-1}) \qquad (26)$$

with the plus sign being taken if $0 < \theta_o < \pi$ and the minus sign if $-\pi < \theta_o < 0$. The second term in equation (26) can be made analytic along $\theta_o = \pi$, but suffers a jump discontinuity across $\theta_o = 0$.

Expansions of the stream function for $\theta_o = 0$ and r_o finite reveal no discontinuity, however. The discontinuity in equation (26) is a property of the asymptotic expansion of $\psi(r_o, \theta_o)$, but not of the stream function itself.

This rather strange behavior can be explained. From equation (10) the vorticity can be shown to behave asymptotically like . . . . .

$$\omega(r,\theta) \sim \frac{e^{-1/2\ Rr\ (1 - \cos\theta)}}{\sqrt{r}} f(\theta) \qquad \text{as } r \to \infty \tag{27}$$

where $f(0) = 0$, $f'(0) \neq 0$. Thus the vorticity decays exponentially as $r \to \infty$ provided $\theta \neq 0$. Along $\theta = 0$, however, we have $\omega(r,0) = 0$ for all r and $\frac{\partial\omega}{\partial\theta}(r,0) = 0\ (r^{-1/2})$ as $r \to \infty$. Thus $\frac{\partial\omega}{\partial\theta}(r,\theta)$ decays algebraically along $\theta = 0$. If $r = L >> 1$, the function $\frac{\partial\omega}{\partial\theta}(L,\theta)$ will be exponentially small as $\theta \to 0$, but will jump to a much larger value when $\theta = 0$ since its decay along this ray is so much slower. This behavior is not unlike a delta function, and, since the stream function is related to the vorticity through Poisson's equation, it is not surprising that a step function behavior appears in the asymptotic expansion of $\psi(r,\theta)$ along $\theta = 0$. It must be stressed, however, that this is a feature of the asymptotics only. The stream function itself is analytic in the fluid domain.

The next term in equation (23) can be calculated and is of the form $\Phi_1(R)r_o^{-1} \sin\theta_o$. In fact, all subsequent terms are of the form $\Phi_k(R)r_o^{-k} \sin k\theta_o$ $(k = 1,2,3,\ldots)$. The asymptotic expansion of the stream function is therefore harmonic (except possibly along $\theta_o = 0$) and gives us the potential flow far from the cylinder. Table 3 contains some computed examples.

BURGERS FLOW AND OSEEN FLOW: HOW DO THEY DIFFER?

The previous section shows that one distinct advantage of a spatially uniform linear approximation to the Navier-Stokes solution is the ability to calculate from it the resulting potential flow at infinity. This potential

Table. 3. Asymptotic expansions for large r.

Oseen Flow			
R = 1.51	$\psi \sim r \sin\theta$	$- 3.3118\left(\pm 1 - \frac{\theta}{\pi}\right)$	$- 0.5995\,\frac{\sin\theta}{r} + O\left(\frac{\sin 2\theta}{r^2}\right)$
R = 2.0		2.9247	0.5777
R = 3.0		2.4888	0.5485
R = 4.0		2.2481	0.5302
R = 5.0		2.0918	0.5171
Burgers Flow			
R = 1.12	$\psi \sim r \sin\theta$	$- 3.6509\left(\pm 1 - \frac{\theta}{\pi}\right)$	$- 1.1251\,\frac{\sin\theta}{r} + O\left(\frac{\sin 2\theta}{r^2}\right)$
R = 2.0		2.6709	1.1396
R = 2.828		2.2327	1.1439
R = 3.464		2.0213	1.1486
R = 4.0		1.8763	1.1467

flow cannot be obtained a priori without some knowledge of the flow near the cylinder because the flow near the cylinder determines the outer edge of the boundary layer, which in turn defines the region of irrotational flow. Without an approximation like Oseen flow or Burgers flow, therefore, the problem of finding $\psi(r,\theta)$ far from the cylinder reduces to finding a harmonic function in a region whose boundary is unknown.

Having obtained the asymptotic expansion given in the previous section, however, it is possible to define the location of the outer edge of the boundary layer as the curve along which this asymptotic expansion vanishes. This amounts to finding a boundary which the potential flow does not penetrate. Slippage along this boundary is, of course, permitted. The boundary so defined determines the displacement body which the potential flow far from the cylinder "sees." The displacement body includes the cylinder, its wake, and the boundary layer surrounding the cylinder.

By setting the asymptotic expansions given in table 3 equal to zero and solving for r, we can obtain approximations to the displacement bodies for the various flows. A typical example is given in figure 6. Note that the displacement body is semi-infinite with its thickness at infinity being twice the value of the $\left(\pm 1 - \frac{\theta}{\pi}\right)$ - coefficient. Since the cylinder boundary is given by $r = 1$, the thickness of the boundary layer is easily calculated. Tables 4 and 5 compile these results for a variety of Reynolds numbers and locations along the cylinder boundary. Note that $\theta = \pi$ refers to the forward stagnation point on the cylinder boundary.

The last column in tables 4 and 5 is a least-squares fit of the data given in each row. In table 4 the value of α depends on θ. In table 5, however, the value of α hovers about $\alpha_0 = 1/2$ regardless of θ. This suggests that the boundary layer thickness is inversely proportional to $R^{1/2}$ in Burgers flow but not in Oseen flow.

Studies of the nonlinear boundary layer flow past a semi-infinite flat plate show unquestionably that the boundary layer thickness behaves like $R^{-1/2}$. Our work obtains a similar result for a bluff body using a linear model in which vorticity is convected around the obstacle's boundary. The agreement between this prediction of Burgers flow and that of nonlinear analysis regarding boundary layer behavior indicates that the Burgers model

Table 4. Boundary layer thickness: Ossen flow.

θ	R = 2.0	R = 3.0	R = 4.0	R = 5.0	$A(\theta)/R^{\alpha}$
π	0.3568	0.2360	0.1691	0.1254	$0.7984/R^{1.1336}$
$\frac{11}{12}\pi$	0.3649	0.2427	0.1750	0.1308	$0.8038/R^{1.1127}$
$\frac{10}{12}\pi$	0.3904	0.2637	0.1936	0.1478	$0.8230/R^{1.0545}$
$\frac{9}{12}\pi$	0.4363	0.3014	0.2270	0.1784	$0.8647/R^{0.9721}$
$\frac{8}{12}\pi$	0.5086	0.3610	0.2796	0.2267	$0.9415/R^{0.8798}$
$\frac{7}{12}\pi$	0.6185	0.4515	0.3597	0.3001	$1.0706/R^{0.7885}$
$\frac{6}{12}\pi$	0.7858	0.5895	0.4818	0.4121	$1.2796/R^{0.7044}$
$\frac{5}{12}\pi$	1.0483	0.8066	0.6743	0.5887	$1.6182/R^{0.6302}$
$\frac{4}{12}\pi$	1.4840	1.1688	0.9962	0.8846	$2.1876/R^{0.5654}$
$\frac{3}{12}\pi$	2.2783	1.8334	1.5892	1.4314	$3.2260/R^{0.5083}$
$\frac{2}{12}\pi$	3.9903	3.2763	2.8834	2.6288	$5.4491/R^{0.4565}$
$\frac{1}{12}\pi$	9.4140	7.8764	7.0282	6.4777	$12.4377/R^{0.4091}$

Table 5. Boundary layer thickness: Burgers flow.

θ	R = 2.0	R = 2.828	R = 3.464	R = 4.0	$A(\theta)/R^{\alpha}$
π	0.5741	0.4823	0.4407	0.4103	$0.8005/R^{0.4825}$
$\frac{11}{12}\pi$	0.5808	0.4878	0.4454	0.4147	$0.8108/R^{0.4841}$
$\frac{10}{12}\pi$	0.6018	0.5045	0.4603	0.4283	$0.8427/R^{0.4886}$
$\frac{9}{12}\pi$	0.6394	0.5347	0.4870	0.4527	$0.9001/R^{0.4962}$
$\frac{8}{12}\pi$	0.6988	0.5823	0.5291	0.4912	$0.9911/R^{0.5069}$
$\frac{7}{12}\pi$	0.7891	0.6545	0.5930	0.5494	$1.1297/R^{0.5205}$
$\frac{6}{12}\pi$	0.9269	0.7646	0.6902	0.6381	$1.3422/R^{0.5368}$
$\frac{5}{12}\pi$	1.1444	0.9385	0.8437	0.7780	$1.6786/R^{0.5552}$
$\frac{4}{12}\pi$	1.5101	1.2314	1.1023	1.0138	$2.2435/R^{0.5734}$
$\frac{3}{12}\pi$	2.1901	1.7797	1.5878	1.4569	$3.2853/R^{0.5867}$
$\frac{2}{12}\pi$	3.6943	3.0067	2.6809	2.4587	$5.5407/R^{0.5858}$
$\frac{1}{12}\pi$	8.5786	7.0497	6.3159	5.8136	$12.6387/R^{0.5598}$

is a substantial improvement over the Oseen model in describing the flow near the cylinder.

BURGERS FLOW PAST AN ELLIPTIC CYLINDER

We consider first the case when the major axis of the ellipse is parallel to the uniform stream at infinity. The appropriate coordinate system is (ξ,η) where

$$x = \cosh \xi \cos \eta$$

$$y = \sinh \xi \sin \eta \tag{28}$$

The curve $\xi = \xi_o$ represents an ellipse with major axis $2 \cosh \xi_o$ along the x-axis and minor axis $2 \sinh \xi_o$. The continuous inviscid potential flow which gives the convective velocity field satisfies the boundary value problem

$$\nabla^2 \psi = 0 \qquad \xi > \xi_o, \quad -\pi < \eta \leq \pi$$

$$\psi(\xi_o,\eta) = 0$$

$$\psi \sim y \sim \frac{1}{2} e^{\xi} \sin \eta \quad \text{as} \quad \xi \to +\infty \tag{29}$$

The solution of equation (29) is

$$\psi(\xi,\eta) = e^{\xi_o} \sinh (\xi - \xi_o) \sin \eta \tag{30}$$

If $\psi(\xi,\eta)$ is the stream function for Burgers flow past an ellipse, the boundary value problem for ψ is defined as follows:

$$\left\{ \frac{\partial^2}{\partial \xi^2} + \frac{\partial^2}{\partial \eta^2} + R \left(\frac{\partial \psi}{\partial \xi} \frac{\partial}{\partial \eta} - \frac{\partial \psi}{\partial \eta} \frac{\partial}{\partial \xi} \right) \right\} \omega(\xi,\eta) = 0 \tag{31}$$

$$\nabla^2\psi \equiv \frac{1}{\cosh^2\xi - \cos^2\eta}\left\{\frac{\partial^2\psi}{\partial\xi^2} + \frac{\partial^2\psi}{\partial\eta^2}\right\} = -\omega(\xi,\eta) \tag{32}$$

$$\psi(\xi_o,\eta) = \frac{\partial\psi}{\partial\xi}(\xi_o,\eta) = 0$$

$$\psi \sim \frac{1}{2} e^{\xi} \sin\eta \quad \text{as} \quad \xi \to \infty \tag{33}$$

The parameter R in equation (31) is proportional to the Reynolds number. Its value is

$$R = \frac{R_s}{\cosh\xi_o} \tag{34}$$

where R_s is the Reynolds number based on the semimajor axis of the ellipse. In the limit $\xi_o \to 0$, the ellipse degenerates to a finite flat plate. Since the potential flow parallel to a flat plate is a uniform stream, Burgers flow and Oseen flow are equivalent when $\xi_o = 0$.

As in the case of the circle, the vorticity function has the form

$$\omega(\xi,\eta) = -e^{\frac{1}{2}R\phi(\xi,\eta)} \sum_{n=1}^{\infty} E_n F_n(\xi) T_n(\eta) \tag{35}$$

where $\phi(\xi,\eta) = e^{\xi_o}\cosh(\xi - \xi_o)\cos\eta$ is the harmonic conjugate of $\Psi(\xi,\eta)$. The resulting ordinary differential equations for $F_n(\xi)$ and $T_n(\eta)$ are different versions of Mathieu's equation with solutions given by

$$F_n(\xi) = \text{Gek}_n\left(\xi - \xi_o, -\frac{1}{16}R^2 e^{2\xi_o}\right)$$

$$T_n(\eta) = \text{se}_n\left(\eta, -\frac{1}{16}R^2 e^{2\xi_o}\right) \tag{36}$$

If we make the following substitutions in equations (35) and (36):

$$z = \xi - \xi_o, \qquad \theta = \eta, \qquad C = \frac{1}{2} R e^{\xi_o} \tag{37}$$

the Burgers vorticity past an ellipse has exactly the same form as that past a circle: namely,

$$\omega(z,\theta) = -e^C \cosh z \cos\theta \sum_{n=1}^{\infty} E_n \, \mathrm{Gek}_n\left(z, -\frac{1}{4}C^2\right) \mathrm{se}_n\left(\theta, -\frac{1}{4}C^2\right) \tag{38}$$

Poisson's equation [eq. (32)] becomes

$$\frac{\partial^2\psi}{\partial z^2} + \frac{\partial^2\psi}{\partial\theta^2} = -\frac{1}{2} h(z,\theta)\, \omega(z,\theta) \tag{39}$$

where

$$h(z,\theta) = \cosh 2(z + \xi_o) - \cos 2\theta \tag{40}$$

and its solution follows the technique described under "Solution." Omitting the details we find

$$\psi(z_o,\theta_o) = e^{\xi_o} \sinh z_o \sin\theta_o + \frac{1}{2} \int_{-\pi}^{\pi} \int_{o}^{\infty} h(z,\theta) \cdot \omega(z,\theta)\, G(z,\theta;z_o,\theta_o)\, dz\, d\theta \tag{41}$$

where

$$G(z,\theta;z_o,\theta_o) = \frac{-1}{4\pi} \ln\left[\frac{\cosh(z - z_o) - \cos(\theta - \theta_o)}{\cosh(z + z_o) - \cos(\theta - \theta_o)}\right]$$

The coefficients E_n in equation (38) satisfy the infinite linear system

$$\sum_{n=1}^{\infty} E_n \Gamma_{kn} = \delta_{kl} \qquad k = 1,2,3,\ldots \tag{42}$$

where

$$\Gamma_{kn} = \frac{e^{-\xi_o}}{\pi} \int_0^{\pi} \int_0^{\infty} h(z,\theta) e^{-k z + C \cosh z \cos\theta}$$

$$\cdot \, \mathrm{Gek}_n\left(z, -\frac{1}{4}C^2\right) \sin k\theta \; \mathrm{se}_n\left(\theta, -\frac{1}{4}C^2\right) dz \, d\theta \tag{43}$$

If the ellipse has its major axis perpendicular to the flow at infinity, a different coordinate system is required. Consider the elliptic coordinates (μ,λ) defined by

$$x = \sinh\mu \cos\lambda$$

$$y = \cosh\mu \sin\lambda \tag{44}$$

The curve $\mu = \mu_o$ represents an ellipse with major axis along the y-axis. The potential flow past this ellipse has stream function $\chi(\mu,\lambda)$ which satisfies exactly those conditions given in equation (29). Thus from equation (30) we have

$$\chi(\mu,\lambda) = e^{\mu_o} \sinh(\mu - \mu_o) \sin\lambda \tag{45}$$

Since the potential flows in equations (30) and (45) are functionally the same, it follows that the Burgers solution in (μ,λ) coordinates will be similar to that in (ξ,η) coordinates. In fact, if the variables (μ,λ,χ) are replaced by (ξ,η,Ψ), the problem is identical with that in equations (31) to (33), except that equation (32) is replaced by

$$\nabla^2\psi \equiv \frac{1}{\sinh^2\xi + \cos^2\eta}\left\{\frac{\partial^2\psi}{\partial\xi^2} + \frac{\partial^2\psi}{\partial\eta^2}\right\} = -\omega(\xi,\eta) \tag{46}$$

It follows that the stream function for Burgers flow past an ellipse whose major axis is perpendicular to the flow is given by equations (41) to (43) where $h(z,\theta)$ is now given by;

$$h(z,\theta) = \cosh 2(z + \xi_o) + \cos 2\theta \tag{47}$$

The research that remains to be done includes a detailed analysis of the elliptical solutions. It is my intention to compute drag coefficients for various elliptical cylinders, examine separation phenomena, and calculate surface pressure distributions. The asymptotic form of the stream function will be used to deduce displacement body shape and boundary layer thickness for various cases. The special cases of the flow past a finite flat plate (both parallel to and perpendicular to the uniform stream) will be considered in detail and compared with experimental data where possible.

REFERENCES

1. Yamada, H.: On the Slow Motion of Viscous Liquid Past a Circular Cylinder. Rep. Res. Inst. Appl. Mech. Kyushu Univ., Vol. 3, 1954, pp. 11-23.

2. Underwood, R.L.: Calculation of Incompressible Flow Past a Circular Cylinder at Moderate Reynolds Numbers. J. Fluid Mech., Vol. 37, 1969, pp. 95-114.

3. Batchelor, G.K.: An Introduction to Fluid Dynamics. Cambridge Univ. Press, 1967, p. 261.

4. Van Dyke, M.: Perturbation Methods in Fluid Mechanics. Parabolic Press, 1975, p. 164.

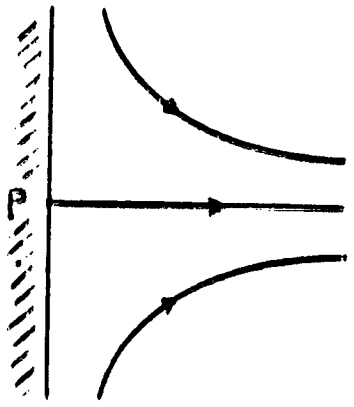

Figure 1.
Streamlines at the rear stagnation point P of the cylinder prior to separation

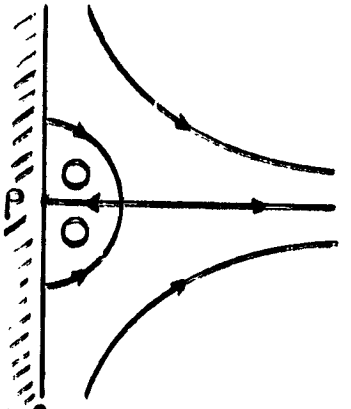

Figure 2.
Streamlines after separation

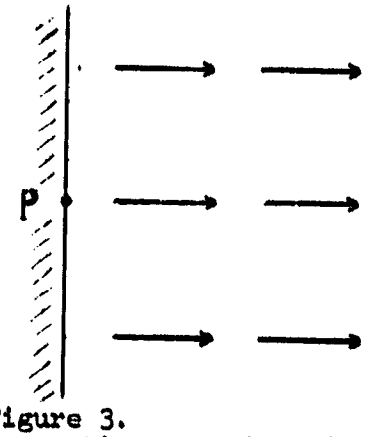

Figure 3.
Convective velocity field at the rear stagnation point of the cylinder in Oseen flow

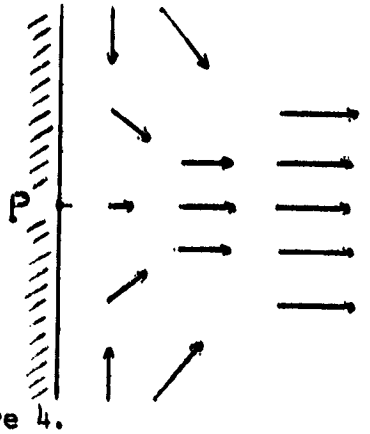

Figure 4.
Convective velocity field in Burgers flow

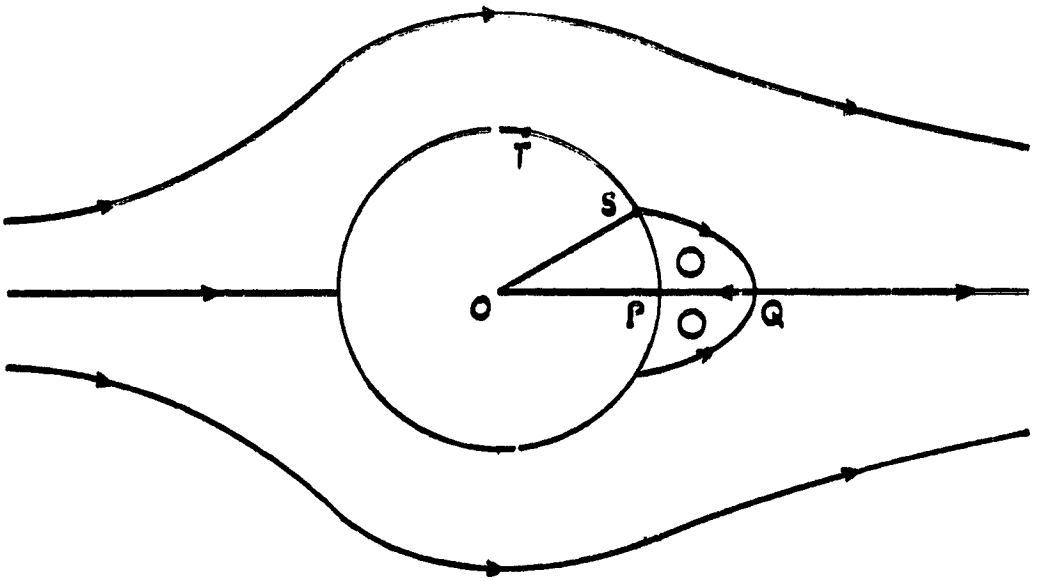

Figure 5. Burgers flow at R=2.0

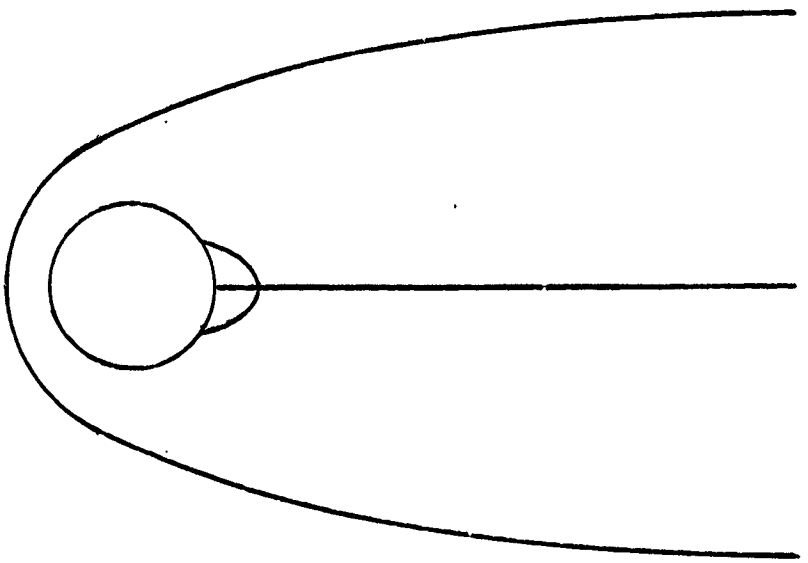

Figure 6.
Displacement body for Burgers flow at R=2.0